Comparison of multigrid and incomplete LU shifted-Laplace preconditioners for the inhomogeneous Helmholtz equation*

Y.A. Erlangga†, C. Vuik, C.W. Oosterlee
Delft Institute of Applied Mathematics, Delft University of Technology
Mekelweg 4, 2628 CD Delft, The Netherlands

February 22, 2005

Abstract

Within the framework of shifted-Laplace preconditioners [*Erlangga, Vuik, Oosterlee, Appl. Numer. Math., 50(2004), pp.409–425*] for the Helmholtz equation, different methods for the approximation of the inverse of a complex-valued Helmholtz operator are discussed. The performance of the preconditioner for Helmholtz problems at high wavenumbers in heterogeneous media is evaluated. Comparison with other preconditioners from the literature is also presented.

Keywords: Helmholtz equation, shifted-Laplace preconditioner, Krylov subspace methods, multigrid, ILU

1 Introduction

Consider the Helmholtz equation for a wave problem in an inhomogeneous medium

$$-\partial_{xx}\phi - \partial_{yy}\phi - k^2(x,y)\phi = g(x,y) \quad \text{in } \Omega \subset \mathbb{R}^2, \tag{1}$$

satisfying the first order radiation boundary condition

$$\frac{\partial \phi}{\partial \eta} - \hat{\jmath} k(x,y)\phi = 0 \text{ on } \Gamma = \partial\Omega, \tag{2}$$

with η the outward direction normal to the boundaries, and $\hat{\jmath} = \sqrt{-1}$ the complex identity. In (1) and (2) $k = k(x,y) \in \mathbb{R}$ is the wavenumber, g is the

*The research is financially supported by the Dutch Ministry of Economic Affairs under the Project BTS01044

†Email address: {y.a.erlangga,c.vuik,c.w.oosterlee}@math.tudelft.nl

source function and $\phi = \phi(x, y)$, the solution, usually represents a pressure wave. In many practical applications, e.g. in geophysics, k can be very large.

We approximate the Laplacian in (1) with the second order accurate 5-point finite difference stencil:

$$L_h \stackrel{\wedge}{=} \frac{1}{h^2} \begin{bmatrix} & 1 & \\ 1 & -4 & 1 \\ & 1 & \end{bmatrix}_h , \tag{3}$$

(in stencil notation) and central differencing for (2). Using this stencil, a linear system of the form

$$Ap = b,\ A \in \mathbb{C}^{N \times N},\ p, b \in \mathbb{C}^N, \tag{4}$$

is obtained where $N = N_x N_y$ is the number of unknowns in the computational domain Ω_h, and N_x and N_y are the number of grid points in the x- and y-directions, respectively. The matrix $A \in \mathbb{C}$ because of boundary condition (2). A is in general symmetric, indefinite, non-Hermitian and, because of accuracy requirements, also large. However, A is sparse; its sparsity pattern depends on the discretization method used.

To solve (4), iterative methods based on the Krylov subspace are of our interest. The methods are cheap to be implemented and are able to exploit the sparsity of A. There are some difficulties for these methods when applied to the Helmholtz equation. First of all, A is typically extremely ill-conditioned. For an ill-conditioned system the convergence of a Krylov subspace method can be unacceptably slow. Secondly, for large wavenumbers k matrix A is highly indefinite. Because for an indefinite linear system the eigenvalues are distributed in the negative and positive half plane, some eigenvalues may lie very close to the origin. This type of spectrum is not favorable for fast convergence of Krylov subspace methods.

To improve their performance, one usually uses a properly chosen preconditioner so that the preconditioned system is better conditioned. Given a matrix $M = M_1 M_2 \in \mathbb{C}^{N \times N}$, by preconditioning one solves the equivalent linear system

$$M_1^{-1} A M_2^{-1} \hat{p} = M_1^{-1} b,\ \ \hat{p} = M_2 p. \tag{5}$$

Since the paper of Bayliss, Turkel, and Goldstein in 1980 [1] much effort has been put in the search for a powerful preconditioner for (4). Without being exhaustive, we refer to [5, 8, 11, 13] for some of these preconditioners.

In general, there are two classes of preconditioners for the Helmholtz equation. The first one is classified as "matrix-based" preconditioners. For this class, M^{-1} is based on an approximation of the inverse of A. Examples in this class are an incomplete LU (or ILU) or an approximate inverse of A. As ILU factors are relatively easily computed, the work in one iteration is cheap. ILU preconditioners, however, may require extra storage due to fill-in and this requirement may exceed that for storing A. Furthermore, ILU factorization may not be stable if A is not an M-matrix.

The second class is the "operator-based" preconditioning. In this class the preconditioner is built based on an operator for which the spectrum of preconditioned system $M^{-1}A$ is favorably clustered. This operator does not have to be a representation of the inverse of the Helmholtz operator. We refer the reader to [12] for a general discussion on this class of preconditioners. Placed within this class are the Analytic ILU (or AILU) [5], the Separation-of-Variables [13] and the Laplace preconditioner [1].

Preconditioning with the Laplace operator [1] for (4) has been enhanced in [9] by adding a positive zero-th order real term with the same Helmholtz constant k^2. In [3] we propose a further generalization and arrive, after some analysis, at a positive *imaginary* shift of the zero-th order term for an improved convergence rate. The class of preconditioners where a zero-th order term has been added to the Laplace operator is called "Shifted-Laplace Preconditioners".

From the formal formulation of preconditioners (5), matrix M should be inverted exactly, e.g., by a direct method. Instead of having M^{-1} exactly, one can construct ILU factors of M and perform only one ILU forward-backward substitution to approximate M^{-1}. Another way to approximate M^{-1} is by using a multigrid iteration.

This paper gives some analysis on the convergence of Krylov subspace methods to solve the Helmholtz equation preconditioned by the shifted-Laplace preconditioner. We show that, based on the GMRES convergence theory, the bound of the convergence rate can be obtained if radiation condition (2) is used. Finally, we compare the *overall* performance of the shifted-Laplace preconditioner with other preconditioners (i.e. Separation-of-Variables [13] and incomplete factorization [11]).

The paper is organized as follows. In Section 2, preconditioned Krylov subspace methods are briefly discussed, alongside with some preconditioners for the Helmholtz equation. Section 3 deals with convergence analysis of Krylov subspace methods for solving the Helmholtz equation preconditioned by the complex shifted-Laplace preconditioner. Multigrid for approximately inverting the shifted-Laplace operator is detailed in Section 4. Numerical examples are presented in Section 5.

2 Preconditioned Krylov Subspace Method

Iterative methods for linear system (4) within the class of Krylov subspace methods are based on the construction of iterants in the subspace

$$\mathcal{K}^j(A, r_0) = \text{span}\{r_0, Ar_0, A^2r_0, \ldots, A^{j-1}r_0\}, \tag{6}$$

where $\mathcal{K}^j(A, r_0)$ is the j-th Krylov subspace associated with A and r_0; $r_0 = b - Ap_0$ is the initial residual. There are many ways to construct the Krylov subspace, which lead to different algorithms. For a survey, see [15].

Since we are interested in a solution method that is not stringent in the choice of preconditioner, we use a Krylov subspace method for unsymmetric

matrices. Bi-CGSTAB [18], despite requiring two matrix-vector multiplications, can preserve a constant amount of work and storage per iteration.

In [3] GMRES [14] is used to solve the Helmholtz equation and is compared with Bi-CGSTAB. Bi-CGSTAB is preferred since the convergence for heterogeneous high wavenumber Helmholtz problems is typically faster than that of GMRES.

In the following subsections, we will shortly discuss some preconditioners for the Helmholtz equation, namely the shifted-Laplace preconditioner (our method of choice), the incomplete factorization of a "modified" Helmholtz operator [11] and the Separation-of-Variables preconditioner [13] (with which we compare our numerical results).

2.1 Shifted-Laplace Preconditioner

The shifted-Laplace (SL) preconditioner is based on the operator

$$\mathcal{M}_{SL} := -\partial_{xx} - \partial_{yy} + \alpha k^2(x,y),\ \alpha \in \mathbb{C}. \tag{7}$$

We consider a particular case where $\mathrm{Re}(\alpha), \mathrm{Im}(\alpha) \geq 0$.

For $\mathrm{Re}(\alpha), \mathrm{Im}(\alpha) > 0$ we find that central differencing of (7) leads to a CSPD matrix M_{SL}. $A \in \mathbb{C}^{N\times N}$ is a complex symmetric, positive definite (CSPD) matrix if both $\mathrm{Re}(A)$ and $\mathrm{Im}(A)$ are SPD.

We have shown in [3] that for $\alpha \neq 0$, $M_{SL}^{-1}A$ has the following properties:

(i) Its eigenvalues are clustered around the origin with $\left|\lambda_{\max}(M_{SL}^{-1}A)\right| \leq 1$,

(ii) The smallest eigenvalues lie close to the origin at a distance $\mathcal{O}(\frac{1}{k})$.

(iii) The minimal condition number $\kappa_{\min}$ in this context is obtained if $\alpha = \hat{\jmath}$, where $\hat{\jmath} = \sqrt{-1}$. For CGNR [15] an immediate conclusion is that choosing $\alpha = \hat{\jmath}$ gives the best CGNR convergence within this class of preconditioners.

We call the version with $\alpha = \hat{\jmath}$ the "complex shifted-Laplace" (CSL) preconditioner. For CSL, the operator (7) now reads

$$\mathcal{M}_{CSL} := -\partial_{xx} - \partial_{yy} + \hat{\jmath} k^2(x,y). \tag{8}$$

Even though the analysis in [3] is only given for constant wavenumber Helmholtz problems in connection with CGNR, numerical results presented show that the analysis results hold for more general Helmholtz problems and other Krylov subspace methods, like GMRES or Bi-CGSTAB.

In Section 4 we detail the analysis of the convergence properties of the Helmholtz equation, preconditioned by (8).

Since M_{CSL} is CSPD, in relation with a CSPD matrix the following lemma is useful. To prove this lemma we recall the *bilinear form* of any real symmetric matrix A, i.e. for any $x, y \in \mathbb{R}$, $x^T Ay = y^T Ax$.

Lemma 1. Let A be any CSPD matrix and let $\lambda_A \in \mathbb{C}$ be an eigenvalue. Then $\mathrm{Re}(\lambda_A), \mathrm{Im}(\lambda_A) > 0$.

Proof. Consider the eigenvalue problem $Av = \lambda_A v$ with v the corresponding eigenvector. Thus, $v^*Av = \lambda_A v^*v$. Using $A = \mathrm{Re}(A) + \hat{j}\mathrm{Im}(A)$ and $v = \mathrm{Re}(v) + \hat{j}\mathrm{Im}(v)$ we have

$$\begin{aligned}\lambda_A v^*v &= \mathrm{Re}(v)^T\mathrm{Re}(A)\mathrm{Re}(v) + \mathrm{Im}(v)^T\mathrm{Re}(A)\mathrm{Im}(v)\\ &+ \hat{j}\left\{\mathrm{Re}(v)^T\mathrm{Re}(A)\mathrm{Im}(v) - \mathrm{Im}(v)^T\mathrm{Re}(A)\mathrm{Re}(v)\right\}\\ &+ \hat{j}\left\{\mathrm{Re}(v)^T\mathrm{Im}(A)\mathrm{Re}(v) + \mathrm{Im}(v)^T\mathrm{Im}(A)\mathrm{Im}(v)\right\}\\ &+ \mathrm{Im}(v)^T\mathrm{Im}(A)\mathrm{Re}(v) - \mathrm{Re}(v)^T\mathrm{Im}(A)\mathrm{Im}(v).\end{aligned}$$

By using the definition of CSPD, the bilinear form and the definition of an SPD matrix, we find that

$$\begin{aligned}\mathrm{Re}(\lambda_A) &= (\mathrm{Re}(v)^T\mathrm{Re}(A)\mathrm{Re}(v) + \mathrm{Im}(v)^T\mathrm{Re}(A)\mathrm{Im}(v))/v^*v > 0,\\ \mathrm{Im}(\lambda_A) &= (\mathrm{Re}(v)^T\mathrm{Im}(A)\mathrm{Re}(v) + \mathrm{Im}(v)^T\mathrm{Im}(A)\mathrm{Im}(v))/v^*v > 0,\end{aligned}$$

which completes the proof. ■

2.2 Incomplete Factorization-Based Preconditioner [11]

An ILU factorization may not be stable if A is not an M-matrix, which is the case for the discrete Helmholtz equation. In [11] approximations of A are proposed so that ILU factorizations can be constructed safely. For the approximation of A^{-1}, denoted by M_I^{-1}, a constraint is set so that the preconditioned system AM_I^{-1} is definite or "less indefinite". Since the term "indefiniteness" is related to the real part of spectrum of the given linear system, one demands that $\mathrm{Re}\left(\sigma(AM_I^{-1})\right) > 0$ (or $\mathrm{Re}\left(\sigma(AM_I^{-1})\right) < 0$).

For $A \in \mathbb{C}$, a matrix $\tilde{A}$ can be extracted from A where the real part of $\tilde{A}$ is a non-singular symmetric M-matrix [17]. In our situation (i.e. the Helmholtz equation discretized by (3)), by introducing a parameter $\gamma \geq 1$ and defining

$$\mathrm{Re}(\tilde{a}_{ij}) = \begin{cases}\mathrm{Re}(a_{ij}) & \text{if } i \neq j,\\ \mathrm{Re}(a_{ij}) - \gamma\min\{0, \mathrm{Re}((Ae)_i)\} & \text{if } i = j,\end{cases}$$

it can be proved that $\mathrm{Re}(\tilde{A})$ is a non-singular symmetric M-matrix [11]. Then, $\mathrm{Re}(\tilde{A})$ can be considered as a real perturbation of $\mathrm{Re}(A)$. Since $\mathrm{Re}(\tilde{A})$ is a symmetric M-matrix, the ILU algorithm can be applied safely. For the imaginary part, one simply sets

$$\mathrm{Im}(\tilde{a}_{ij}) = \mathrm{Im}(a_{ij}),\ \forall i, j.$$

In [11] several possible settings for this preconditioner are proposed. Here, we only evaluate one of them, namely

$$M_I \equiv \tilde{A} = A_0 + \hat{j}\mathrm{Im}(A),\ \ A_0 = \mathrm{Re}(A) + Q, \tag{9}$$

with

$$q_{ii} = -\min\{0, \mathrm{Re}((Ae)_i)\}, \ \ (\gamma = 1). \tag{10}$$

2.3 Separation-of-Variables Preconditioner [13]

It is well known that a separation of variables technique can be used to analytically solve the Laplace equation with special boundary conditions. The zeroth order term $k^2(x,y)u$ prevents the use of this technique for the Helmholtz operator. An approximation can, however, be made in the separation of variables context. This approximation can be used as a preconditioner for the Helmholtz equation.

For $k^2(x,y)$ an arbitrary twice integrable function, the following decomposition can be made,

$$k^2(x,y) = k_x^2(x) + k_y^2(y) + \tilde{k}^2(x,y), \ \ \text{in} \ \ \Omega = [x_a, x_b] \times [y_a, y_b], \tag{11}$$

satisfying the conditions

$$\int_{x_a}^{x_b} \tilde{k}^2(x,y)dx \ \ = \ \ 0, \ \ \forall y, \int_{y_a}^{y_b} \tilde{k}^2(x,y)dy = 0, \ \ \forall x.$$

It can be proved that the decomposition (11) is unique [13]. Denoting by K, a matrix representation of the zero-th order term, and L_Δ, the Laplace term, matrix A can be written as

$$A = L_\Delta - K^2 = X + Y - K^2, \tag{12}$$

where

$$X \ \ = \ \ I_y \otimes A_x, \ \ Y = A_y \otimes I_x, \ \text{and} \ K^2 = I_y \otimes K_x^2 + K_y^2 \otimes I_x + \widetilde{K^2},$$

with $\otimes$ the Kronecker product, I_x, I_y identity matrices and $K_x^2, K_y^2, \widetilde{K^2}$ diagonal matrices related to (11).

It is $\tilde{k}$ in (11) which prevents a complete decomposition of A. If we neglect this term, K^2 can be decomposed in the same way as L_Δ. This results in the following separated variables formulation

$$\widehat{A} := X + Y - \widehat{K^2} = I_y \otimes (A_x - K_x^2) + (A_y - K_y^2) \otimes I_x, \tag{13}$$

where $\widehat{A}$ approximates A up to the term $\widetilde{K^2}$. If wavenumber k is constant then decomposition (11) is exact. As $\widehat{A}$ can be further decomposed into a block tridiagonal matrix, it is motivating to use $\widehat{A}$ as a preconditioner for A. We denote this preconditioner throughout this paper by $M_{SV} := \widehat{A}$.

The construction of a block tridiagonal decomposition of M_{SV} involves the singular value decomposition in one direction, e.g. in the x-direction. We refer to [13] for more details.

3 Analysis of Shifted-Laplace Preconditioner

In this section we give some convergence analysis for the discrete Helmholtz equation, preconditioned by the complex shifted-Laplace preconditioner. We first provide the spectral properties of a Helmholtz problem with Dirichlet boundary conditions (called "closed-off problem"). In Section 3.2, we use the results to obtain a bound for the convergence rate of GMRES for Helmholtz problems with radiation condition (2). In the analysis, we need to set wavenumber k constant.

3.1 Closed-off Problem

The "closed-off" Helmholtz problem analyzed is defined as follows:

$$\begin{aligned} -\frac{\partial^2\phi}{\partial x^2} - \frac{\partial^2\phi}{\partial y^2} - k^2\phi &= 0, \text{ in } \Omega = (0,1)^2, & (14)\\ \phi(0,y) = \phi(1,y) &= 0, \phi(x,0) = \phi(x,1) = 0. & (15) \end{aligned}$$

The eigenvalue problem related to (14)-(15) reads

$$\begin{aligned} \left(-\frac{\partial^2}{\partial x^2} - \frac{\partial^2}{\partial y^2} - k^2\right) v^{m,n} &= \lambda_{mn} v^{m,n}, \ \ m,n \in \mathbb{Z} & (16)\\ v^{m,n}(0,y) = v^{m,n}(1,y) &= 0, & (17)\\ v^{m,n}(x,0) = v^{m,n}(y,1) &= 0, & (18) \end{aligned}$$

where $v^{m,n}$ and λ_{mn} are the eigenfunctions and eigenvalues, respectively. The eigenfunctions

$$v^{m,n} = \sin(m\pi x)\sin(n\pi y), \quad \text{for} \ \ m,n \in \mathbb{Z}. \tag{19}$$

satisfy (16)-(18). Substituting these eigenfunctions in (16) yields

$$\lambda_{mn} = k_m^2 + k_n^2 - k^2,\ k_m = m\pi,\ k_n = n\pi. \tag{20}$$

In this case k_m, k_n are the natural frequencies. Resonance occurs if the wavenumber (or reduced frequency), k, is equal to $k_{mn} := \sqrt{k_m^2 + k_n^2}$. It resembles the condition $\lambda_{mn} = 0$.

Now, the complex shifted-Laplace preconditioner (8) is used to speed up the convergence. Using the boundary conditions (15), we can write the preconditioned eigenvalue problem as

$$-\left(\frac{\partial^2}{\partial x^2} + \frac{\partial^2}{\partial y^2} + k^2\right) v^{m,n} = \lambda_{mn}^p \left(-\frac{\partial^2}{\partial x^2} - \frac{\partial^2}{\partial y^2} + \hat{\jmath} k^2\right) v^{m,n}. \tag{21}$$

With a solution of the form (19), one can show that the eigenvalues are now distributed according to

$$\lambda_{mn}^p = \frac{k_m^2 + k_n^2 - k^2}{k_m^2 + k_n^2 + \hat{\jmath} k^2},\ k_m = m\pi,\ k_n = n\pi,\ n,m \in \mathbb{Z}. \tag{22}$$

This means that the preconditioned system is still indefinite as there is a possibility that $k_m^2 + k_n^2 - k^2$ changes sign, but now with a clustered spectrum.

Let us identify the complex plane with the usual Cartesian plane. In this Cartesian plane, we identify $\mathrm{Re}(\lambda^p)$ and $\mathrm{Im}(\lambda^p)$ as two variables x and y, respectively. Adding up $\mathrm{Re}(\lambda^p)$ and $\mathrm{Im}(\lambda^p)$ we find that

$$\mathrm{Re}(\lambda_{mn}^p) + \mathrm{Im}(\lambda_{mn}^p) = (k_{mn}^2 - k^2)^2/(k_{mn}^4 + k^4). \tag{23}$$

Assume that resonance does not occur. We can conclude that $\mathrm{Re}(\lambda^p)+\mathrm{Im}(\lambda^p) > 0$. This analysis gives the following result.

Lemma 2. Let the 2D Helmholtz equation (14) with boundary conditions (15) be preconditioned by (8), giving a corresponding spectrum. If resonance does not occur, then for all $k^2 \neq k_{mn}^2$ the convex hull of the spectrum does not intersect the line $\mathrm{Re}(z) + \mathrm{Im}(z) = 0$. More specifically, the spectrum then completely lies above this line.

This lemma suggests a rotation of the spectrum so that, based on this line, the eigenvalues become "definite" (all eigenvalues are translated to the left/right complex half plane). From Lemma 2 it is also known that this line is at an angle $\theta = \frac{\pi}{4}$ with the imaginary axis (Figure 1). We define the z_θ-plane by using the transformation

$$\lambda_\theta^p = \lambda^p \exp(\hat{j}\theta) \tag{24}$$

and (22) obtain, after some arithmetics,

$$\mathrm{Re}(\lambda_{\theta,mn}^p) = \left(\frac{k_{mn}^2 - k^2}{k_{mn}^4 + k^4}\right)\left(k_{mn}^2 \cos\theta + k^2 \sin\theta\right), \tag{25}$$

$$\mathrm{Im}(\lambda_{\theta,mn}^p) = \left(\frac{k_{mn}^2 - k^2}{k_{mn}^4 + k^4}\right)\left(k_{mn}^2 \sin\theta - k^2 \cos\theta\right), \tag{26}$$

where $k_{mn}^4 = (k_m^2 + k_n^2)^2$.

The condition $\mathrm{sign}(\mathrm{Re}(\lambda_{\theta,mn}^p)) > 0$ for all k_{mn} and k is satisfied only if $\theta = -\pi/4$, yielding

$$\mathrm{Re}(\lambda_{-\frac{\pi}{4},mn}^p) = \frac{1}{2}\sqrt{2}\frac{(k_{mn}^2 - k^2)^2}{k_{mn}^4 + k^4} > 0, \forall k_{mn}, k \tag{27}$$

$$\mathrm{Im}(\lambda_{-\frac{\pi}{4},mn}^p) = -\frac{1}{2}\sqrt{2}\frac{k_{mn}^4 - k^4}{k_{mn}^4 + k^4}. \tag{28}$$

With a ($\theta = -\pi/4$)-rotation one finds that the imaginary part of eigenvalue after rotation, $\mathrm{Im}(\lambda_{-\frac{\pi}{4},mn})$, is positive if $k_{mn}^4 < k^4$.

Eliminating k_{mn} from both equations yields

$$(\mathrm{Re}(\lambda_{-\frac{\pi}{4},mn}^p) - \frac{1}{2}\sqrt{2})^2 + \mathrm{Im}(\lambda_{-\frac{\pi}{4},mn}^p)^2 = \frac{1}{2}, \tag{29}$$

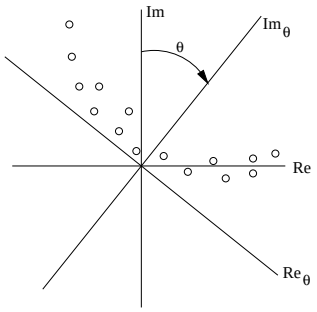

Figure 1: Rotation of the z-plane.

or

$$\left|\lambda^p_{-\frac{\pi}{4},mn} - \frac{1}{2}\sqrt{2}\right| = \frac{1}{2}\sqrt{2}, \tag{30}$$

which leads to the following lemma.

Lemma 3. Let the 2D Helmholtz problem (14) with boundary conditions (15) be preconditioned by (8) and assume that resonance does not occur. Furthermore, let a rotation matrix of the form (24) be introduced. For $\theta = -\pi/4$, the spectrum satisfies the following properties:

(i) All eigenvalues lie on a circle with center $z_{c,-\frac{\pi}{4}} = \frac{1}{2}\sqrt{2}$ and radius $r = \frac{1}{2}\sqrt{2}$. The circle contains the origin but the eigenvalues do not lie exactly at the origin.

(ii) This circle is independent of wavenumber k.

Figure 2 illustrates the results from Lemma 3. As seen, the eigenvalues lie on the circle $|z_\theta - \frac{1}{2}\sqrt{2}|^2 = \frac{1}{2}\sqrt{2}$ for any value of k (the right figure). The grid size affects the position of the small eigenvalues, which asymptotically move closer to the origin. As the circle contains the origin, the classical bound for GMRES can not be used to estimate the convergence. Furthermore, this result requires a closer look at the eigenvalues in the vicinity of the origin if one wants to estimate the convergence. On the other hand, it also implies that if an eigenvalue close to the origin is well approximated by a Ritz value, the convergence of GMRES becomes superlinear [20], which is observed in previous numerical experiments (see [3]).

From Lemma 3, we get the following corollary.

Corollary 4. Let the 2D Helmholtz problem (14) with boundary conditions (15) be preconditioned by (8). Then, the spectrum lies on the circle

$|z - z_c| = \frac{1}{2}\sqrt{2}$, with $z_c = \frac{1}{2}(1 + \hat{j})$ the center of circle. This circle touches the origin.

Proof. The proof can be obtained by back transformation of the result in Lemma 3 by using the rotation matrix (25) with $\theta = \pi/4$. ■

Remark 5. The introduction of rotation (24) is equivalent to solving the system $PM_{CSL}^{-1}Ax = PM_{CSL}^{-1}b$ with $P = \frac{1}{2}\sqrt{2}\text{diag}(1 + \hat{j})$. The addition of the rotation is not necessary if Krylov subspace algorithms like GMRES or Bi-CGSTAB are used. These methods are able to handle this type of spectrum automatically. Under rotation (25) the condition number κ remains the same, so the GMRES or Bi-CGSTAB convergence does not change.

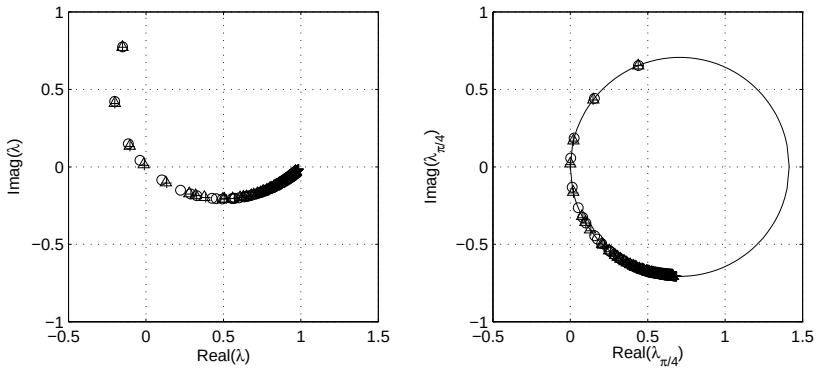

Figure 2: Spectrum of the 2D Helmholtz problem preconditioned with the complex shifted-Laplace preconditioner before (left) and after (right) rotation, Dirichlet boundary conditions, $k = 10$. Grid points: $10(\circ)$, $20(\triangle)$, $30(+)$.

3.2 Analysis for Radiation Boundary Conditions

We consider again the Helmholtz equation (14) preconditioned by (8), but now with the radiation boundary condition (2), and discretize with central differences. One can show that the discretization of the Laplacian and the boundary conditions results in a CSPD matrix $L_\Delta \in \mathbb{C}$ for all $kh > 0$. We introduce the splitting

$$A = L_\Delta - K^2 \iff C := K^{-1}L_\Delta K^{-1} = K^{-1}AK^{-1} + I, \tag{31}$$

where $K = kI, k > 0$. For L_Δ a CSPD matrix we also have that $C = K^{-1}L_\Delta K^{-1} = (kI)^{-1}L_\Delta(kI)^{-1} = k^{-2}L_\Delta$, is a CSPD matrix. From Lemma 1, if λ_C is an eigenvalue of C, then $\text{Re}(\lambda_C), \text{Im}(\lambda_C) > 0$.

We now consider a similar splitting: $M_{CSL} := L_\Delta + \hat{j}K^2$, with boundary condition (2) included in the discretization. For the preconditioned system we

have

$$M_{CSL}^{-1}Av = \lambda_{M_{CSL}^{-1}A}v.$$

It is easy to show that

$$\lambda_{M_{CSL}^{-1}A} = \frac{\lambda_C - 1}{\lambda_C + \hat{j}}. \tag{32}$$

With this result, we obtain the following theorem.

Theorem 6. Let $\lambda_{M^{-1}A}$ be an eigenvalue of $M_{CSL}^{-1}A$, obtained from (8) with boundary condition (2). Let $|z - z_c| = \frac{1}{2}\sqrt{2}$ with $z_c = \frac{1}{2}(1 + \hat{j})$ be the circle corresponding to all eigenvalues of the "closed-off" problem (as described in Corollary 4). Then, $\lambda_{M^{-1}A}$ is enclosed by this circle.

Proof. By using (32) and Corollary 4 we have that

$$\begin{aligned}
\lambda_{M^{-1}A} - z_c &= \frac{\lambda_C - 1}{\lambda_C + \hat{j}} - \frac{1}{2}(1 + \hat{j}) \\
&= \frac{1}{2}\frac{\lambda_C - 1 - \hat{j}(\lambda_C + 1)}{\lambda_C + \hat{j}} \\
&= \frac{1}{2}\frac{(\lambda_C - 1 - \hat{j}(\lambda_C + 1))(\overline{\lambda}_C - \hat{j})}{(\lambda_C + \hat{j})(\overline{\lambda}_C - \hat{j})}.
\end{aligned}$$

With $|\lambda_{M^{-1}A} - z_c|^2 = (\lambda_{M^{-1}A} - z_c)\overline{(\lambda_{M^{-1}A} - z_c)}$, we find that

$$\begin{aligned}
|\lambda_{M^{-1}A} - z_c| &= \frac{1}{2}\sqrt{2}\sqrt{\frac{\lambda_C - \hat{j}}{\overline{\lambda}_C - \hat{j}} \cdot \frac{\overline{\lambda}_C + \hat{j}}{\lambda_C + \hat{j}}} \\
&= \frac{1}{2}\sqrt{2}\sqrt{\frac{\lambda_C\overline{\lambda}_C - 2\mathrm{Im}(\lambda_C) + 1}{\lambda_C\overline{\lambda}_C + 2\mathrm{Im}(\lambda_C) + 1}} < \frac{1}{2}\sqrt{2}
\end{aligned}$$

for every λ_C because of Lemma 1. Therefore, the eigenvalue $\lambda_{M^{-1}A}$ lies inside the circle. This completes the proof. ■

Figure 3 shows eigenvalues before and after a rotation for $k = 10$ and various grid sizes. For all cases, the eigenvalues are enclosed by the circle. The eigenvalues tend to be more clustered for h increasing. In Figure 4 the eigenvalues are shown for different values of k. With increasing k the smallest eigenvalues move closer to the origin.

In terms of convergence analysis, the result with the radiation boundary conditions is stronger than that with the Dirichlet conditions. If rotation (24) is now applied in the context of Theorem 6, we can estimate the convergence bound of GMRES [14].

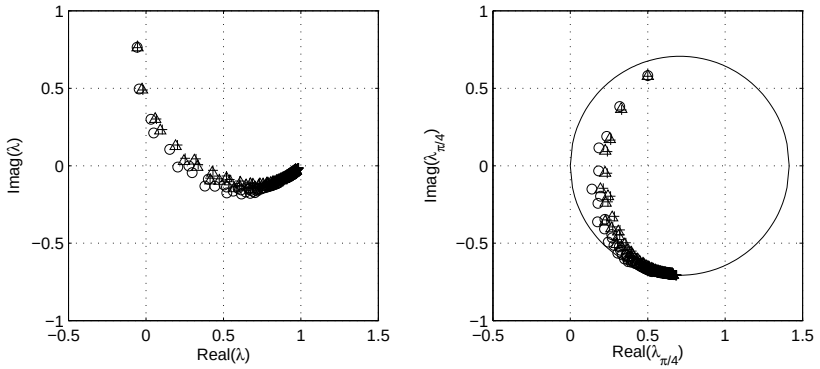

Figure 3: Spectrum of the 2D Helmholtz problem ($k = 10$) with radiation boundary conditions, preconditioned by the complex shifted-Laplace preconditioner before (left) and after (right) rotation. Number of grid points: $10(\circ)$, $20(\triangle)$, $30(+)$.

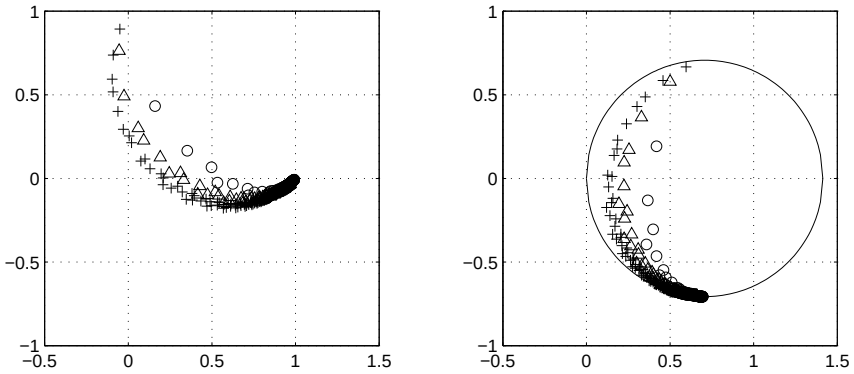

Figure 4: Spectrum of the 2D Helmholtz problem (20^2 grid points) with radiation boundary conditions, preconditioned by the complex shifted-Laplace preconditioner before (left) and after (right) rotation, $k = 5(\circ)$, $k = 10(\triangle)$, $k = 15(+)$.

By $\widetilde{\lambda}^{-\pi/4}_{M^{-1}A} = \max\left|\lambda^{-\pi/4}_{M^{-1}_{CSL}A} - \frac{1}{2}\sqrt{2}\right|$ we denote the eigenvalue of $M^{-1}A$ farthest from the center of the circle after rotation. The circle with center $|z - 1/2| = (\widetilde{\lambda}^{-\pi/4}_{M^{-1}A})^{\frac{1}{2}}$ encloses the remaining eigenvalues but does not contain the origin. From [14] the norm of the residual at the j-th GMRES iteration is then bounded by: $\|r_j\|_2 \leq \left(\frac{R}{C}\right)^j \|r_0\|_2$, with $\kappa(X) = 1$ (we take the eigenvectors of $M^{-1}_{CSL}A$ to determine X). Because of Theorem 6, the rate of convergence of

GMRES can now be bounded by

$$0 < \frac{R}{C} = \frac{(\widetilde{\lambda}_{M^{-1}A}^{-\pi/4})^{\frac{1}{2}}}{\frac{1}{2}\sqrt{2}} < 1. \tag{33}$$

The convergence bound (33) guarantees that GMRES always converges if applied to $M_{CSL}^{-1}A$ with radiation conditions.

4 Solution of Preconditioner

We approximate M^{-1}, the CSL preconditioner (8) by iteration so that the approximation can be obtained cheaply. In particular incomplete LU factorizations and multigrid are evaluated.

4.1 ILU for Shifted-Laplace Operator

An incomplete LU (ILU) factorization can be obtained by computing a sparse lower triangular matrix L and upper triangular matrix U from which the residual matrix $R = LU - A$ satisfies certain constraints. The construction of L and U depends on the Gauss elimination. Since a Gauss elimination always introduces fill-in, the pattern of allowable fill-in determines the accuracy of the LU factors. It is therefore possible that building LU factors may become expensive in storage. Once the LU factors are obtained, the solution can be obtained by forward-backward substitution.

The simplest form of ILU factorization is ILU without fill-in, denoted by ILU(0), where L and U have the same zero pattern as the lower and the upper triangular part of A. ILU(n_{lev}) is obtained if n_{lev} extra fill-in diagonals are allowed in both factors. For this class of ILU factorization, a fast algorithm suitable for matrices with a regular structure stemming, e.g., from finite differencing can be developed. The algorithm is based on some recurrence process and necessitates a minimal extra storage for some entries of the LU factors. For ILU(0), for example, only diagonal components of the lower triangular matrix must be stored. Reference [15] presents a detailed discussion on this subject. In our numerical examples, only ILU(0) and ILU(1) are used.

4.2 Multigrid for Shifted-Laplace Operator

Multigrid is a powerful method for solving an SPD system. It has the nice property that the convergence is independent of the grid size. The use of multigrid in our application becomes attractive since the CSL preconditioner belongs to the class of CSPD matrices. Applications of *algebraic* multigrid for a CSPD system are already presented, e.g., in [10]. Because of its simplicity, we choose *geometric* multigrid and incorporate it inside the Bi-CGSTAB algorithm.

A multigrid method is developed based on two basic principles [16]. First of all, many iterative methods have a strong error smoothing effect if appropriately

applied to discrete elliptic problems. Secondly, a smooth error term is well represented on a coarser grid where its approximation is less expensive than on the finer grid.

The performance of a multigrid method depends on its components. Various multigrid components are discussed in [16] and are used for real-valued linear systems. We implement the same multigrid components for our complex symmetric, positive definite preconditioners and investigate their performance.

As the smoother we use Gauss-Seidel with red-black ordering, denoted by GS-RB. It is, of course, able to handle a complex diagonal element as a natural generalization. For the prolongation operator $I_H^h : \mathcal{G}_H \rightarrow \mathcal{G}_h$, we investigate the matrix-dependent (MD) interpolation proposed by de Zeeuw in [21]. For the restriction operator $I_h^H : \mathcal{G}_h \rightarrow \mathcal{G}_H$, the full weighting operator (FW) is proposed. The coarse grid approximation is done by the Galerkin coarse grid (GCC) approximation, namely $M_H = I_h^H M_h I_H^h$, with M_h and M_H, the matrices corresponding to the fine and coarse grid, respectively. Here we have dropped the subscript "CSL" from the notation M_{CSL} to simplify the notation and to allow the use of subscripts "h" and "H" (that denote the fine and the coarse grid, respectively). Thus, M_h and M_H should be understood as the fine and the coarse grid matrix representation of $\mathcal{M}_{CSL}$. With the transfer operators chosen, the coarse grid matrix is represented by a compact, nine-point stencil. Furthermore, the fine and coarse grid matrices are symmetric.

4.2.1 Two-grid Convergence Analysis

In this section we provide analysis of multigrid convergence for the discrete preconditioning operator M_{CSL}. There are several approaches to analyze multigrid convergence. For example, Hackbusch [6] gives analysis of multigrid based on the *approximation and smoothing* properties of a multigrid method. This approach gives, though important, *qualitative* results. On the other hand, we are interested in *quantitative* estimates of the multigrid convergence. The two-grid Rigorous Fourier Analysis (RFA) [16] is the primary tool in our multigrid analysis. For a symmetric operator like (8) with homogeneous Dirichlet boundary conditions and constant k, we can use the discrete sine-eigenfunctions $v^{m,n}$ (15), $m, n = 1, \ldots, \sqrt{N} - 1$ as the basis for RFA. For two-grid analysis one considers the *two-grid* operator

$$T_h^H = S_h^{\nu_1} C_h^H S_h^{\nu_2}, \text{ with } C_h^H = I_h - I_H^h M_H^{-1} I_h^H M_h. \tag{34}$$

S_h is the smoothing operator on the fine grid, applied ν_1 times before and ν_2 times after the coarse grid correction.

The sine-eigenfunctions are not eigenfunctions of the RB-GS smoother and the two-grid operator T_h^H. The harmonics

$$E_h^{m,n} = \left[v^{m,n}, v^{\sqrt{N}-m,\sqrt{N}-n}, -v^{\sqrt{N}-m,n}, -v^{m,\sqrt{N}-n} \right] \text{ for } m, n = 1, \ldots \sqrt{N}/2 \tag{35}$$

are, however, invariant under this operator. T_h^H can therefore be represented

by a block-diagonal matrix, $\widetilde{T}_h^H$, namely

$$T_h^H \triangleq \left[\widehat{T}_h^H(m,n)\right]_{m,n=1,\ldots,\sqrt{N}/2} =: \widetilde{T}_h^H. \tag{36}$$

The blocks $\widehat{T}_h^H(m,n)$ are 4×4 matrices if $m,n < \sqrt{N}/2$, 2×2 matrices if either $m = \sqrt{N}/2$ or $n = \sqrt{N}/2$, and 1×1 matrices if $m = n = \sqrt{N}/2$. The two-grid convergence factor is defined as

$$\rho_{2g} := \max_{1\le m,n\le \frac{\sqrt{N}}{2}} \rho\left(\widehat{T}_h^H(m,n)\right). \tag{37}$$

One requires to determine the spectral radii of at most 4×4 matrices $\widehat{T}_h^H(m,n)$, and their maximum with respect to m and n.

Table 1 shows RFA results for the preconditioning operator (8) for a constant wave number $k = 100$, $\Omega = (0,1)^2$ and a 256^2 equidistant grid. In the table we show the two-grid convergence factor ρ_{2g}, and the numerical multigrid convergence, ρ_h. In addition, we compute the two-grid operator norm $\|T_h^H\|_S = \sqrt{\rho(T_h^H(T_h^H)^*)}$, to quantify an upper bound for the error reduction in only one multigrid iteration. This latter quantity is interesting since the method is used as a preconditioner and only one multigrid iteration is applied each Krylov subspace iteration.

The multigrid V-cycle is used with the GS-RB smoother, and with the MD-FW transfer operators. The matrix-dependent prolongation operator may be particularly important if a heterogeneity is present in the medium. For constant k the multigrid convergence resembles that of the bilinear interpolation prolongation operator. The V(1,0)-cycle is compared to V(1,1), where in the brackets the number of pre- and post-smoothing steps are indicated. From RFA, the asymptotic two-grid convergence factor for the V(1,1)-cycle is about 0.06, which is in a good agreement with the numerical convergence. Furthermore, the norm of the two-grid operator is well below 0.2. Multigrid for the complex Helmholtz operator (8) behaves very similarly as for the definite real version of the Helmholtz operator (and for the Laplace operator).

Table 1: Asymptotic two-grid and numerical convergence, ρ_{2g} and ρ_h for the preconditioning operator (8), GS-RB smoother. $\|T_h^H\|_S$ is the spectral norm, $N = 256^2$.

Cycle	k	$\|T_h^H\|_S$	ρ_{2g}	ρ_h
V(1,0)	100	0.56	0.25	0.235
V(1,1)	100	0.14	0.063	0.055

One remark should be made here. Starting with the 5-point stencil (3) on the finest grid, the Galerkin coarse grid correction based on matrix-dependent (or bilinear) interpolation and full-weighting restriction results in 9-point coarse

grid stencils. The work on the coarse grids can be substantially reduced if the coarse grid stencil is based on a 5-point stencil. A 5-point coarse grid stencil can be recovered if full-weighting is replaced by half (or full) injection [16]. The RFA results and the actual experiments, however, show that this combination leads to a *diverging* multigrid method for (8), although the method is suitable for the Laplace operator [16].

Table 2 presents the number of multigrid iterations to solve (8) with varying k, and the CPU time for $k = 100$. The transfer operators are MD and FW. The results are presented for a V-cycle with different numbers of pre- and post-smoothing. By increasing the number of pre- and post-smoothing iterations, the number of multigrid iterations to converge can be reduced, but, of course, the CPU time for one cycle increases.

Table 2: Number of multigrid V-cycles to solve the preconditioner (8), with MD and FW as the transfer operators. The CPU time is presented for $k = 100$.

	k					time
(ν_1, ν_2)	20	40	60	80	100	(sec)
(1,0)	9	9	9	9	9	1.01
(1,1)	7	8	6	8	8	1.07
(2,1)	4	6	8	5	6	1.16
(1,2)	4	4	7	4	5	0.97

Since we use multigrid as a method to approximately invert the preconditioner M in the Bi-CGSTAB algorithm, we only consider V(1,0) and V(1,1) in our numerical experiments in Section 5.

5 Numerical Experiments

Numerical tests are performed on three cases which mimic geophysical problems. We start with a relatively simple problem with constant k and increase the difficulty of the problem to a heterogeneous medium, the so-called Marmousi problem.

Bi-CGSTAB with right preconditioning is implemented. For the preconditioner solves, two scenarios are implemented: incomplete LU factorization and multigrid. The iteration is terminated at the q^{th} iteration if the residual satisfies condition $\|r_q\|_2/\|b\|_2 < 10^{-6}$.

All computations are performed on an Intel Pentium 4, 2.6 GHz processor with 512 Mb of RAM. The code is compiled with FORTRAN g77 on LINUX. We use the following notation to indicate the different preconditioners implemented.

(1) ILU(A,n_{lev}) : n_{lev} level ILU applied to the original matrix A,

(2) ILU(M_I,n_{lev}) : n_{lev} level ILU applied to M_I (equations (9) and (10)),

(3) ILU(M_{CSL},n_{lev}) : n_{lev} level ILU applied to M_{CSL} from (8),

(4) MG(V,ν_1,ν_2) : multigrid applied to M_{CSL} with V-cycle, ν_1 pre-smoothing and ν_2 post-smoothing steps,

(5) M_{SV} : Separation-of-Variables preconditioner (13).

Case 1: Constant k. We consider a square domain $\Omega = (0,1)^2$ with a homogeneous medium. The boundaries satisfy the Sommerfeld conditions. A point source is located in the center of the domain. The numerical performance of the different preconditioners for Bi-CGSTAB is shown in Table 3 for increasing k.

All preconditioners accelerate the convergence compared to the unpreconditioned case. Using ILU as the preconditioner based on A, M_I, and M_{CSL} results in a comparable performance here. Further convergence acceleration w.r.t. the number of iterations is achieved by multigrid, especially for k increasing. For example, in case of $k = 100$, the number of iterations is reduced by factor of 4 compared to ILU(1). MG(V(1,0)) improves the CPU time by factor of 2 as compared to ILU(0), but not much gain in CPU time is observed in comparison with ILU(1).

Table 3: Numerical results for a constant k Helmholtz problem. Number of iterations and (between parentheses) CPU time in sec. are shown for various k.

k	10	20	30	40	50	100
grid	32^2	64^2	96^2	128^2	192^2	384^2
No-Prec	150(0.03)	846(0.9)	1577(5.5)	1857(15.3)	3054(59)	6283(483)
ILU(A,0)	75(0.04)	221(0.5)	354(2.3)	474(6.2)	634(19)	1340(159)
ILU(A,1)	35(0.02)	113(0.3)	198(1.5)	238(3.5)	295(10)	563(77)
ILU(M_I,0)	79(0.04)	221(0.5)	394(2.4)	475(6.0)	763(22)	1352(152)
ILU(M_I,1)	42(0.03)	132(0.4)	212(1.4)	238(3.3)	351(11)	577(73)
ILU(M_{CSL},0)	60(0.03)	188(0.5)	334(2.1)	421(5.5)	684(20)	1293(153)
ILU(M_{CSL},1)	36(0.02)	100(0.3)	148(1.1)	206(3.0)	301(10)	536(72)
MG(V(1,0))	18(0.02)	36(0.2)	53(0.8)	63(2.9)	71(7)	133(65)
MG(V(1,1))	16(0.02)	33(0.2)	49(0.9)	60(3.7)	70(9)	133(89)

Case 2: Wedge model. A problem of intermediate difficulty, the wedge model, is used to evaluate the behavior of the preconditioners for a simple heterogeneous medium (see Figure 5). The problem is adopted from [13] so that we can include the numerical results obtained from the Separation-of-Variables preconditioner. The domain is defined as a rectangle of dimension $600 \times 1000\, m^2$. The Sommerfeld boundary conditions are set, and a point source is located at the center of the upper surface (which is assigned to be $y = 0$) with frequency, $f = kc/(2\pi)$, varying from 10 to 50 Hz (with c is the speed of sound). The presence of the heterogeneity brings a variation in c due to different local properties of the medium. The convergence results are presented in Table 4 and an example of the solution for $k = 20$ Hz is in Figure 5.

A similar convergence behavior as for Case 1 is observed; ILU can improve the convergence. Multigrid can further accelerate the convergence as compared

to ILU(0) and ILU(1) but is in CPU time comparable to ILU(1) and tends to be as fast as ILU(M_{CSL},1) for high k. Complex arithmetic operations for the coarse grid nine-point stencil elements may be the reason for the comparable CPU time of multigrid and ILU(M_{CSL},1).

The use of a V-cycle with only a pre-smoothing step for the preconditioner is the best option w.r.t. multigrid; The combination Bi-CGSTAB and ILU(1) for M_{CSL} solves the problem fastest among the choices presented. For high frequencies, the complex shifted-Laplace preconditioner M_{CSL} does not show any breakdown of the iterations, whereas the SV preconditioner did (CPU time is not given for SV in [13]). The performance of the complex shifted-Laplace preconditioner behaves well; the number of iterations increases almost linearly against f.

Case 3: Marmousi problem. The last example is the Helmholtz equation in a part of the Marmousi problem which mimics subsurface geology (see Figure 6). The domain is taken to be rectangular with a dimension of $6000 \times 1600\ m^2$. The Sommerfeld conditions are imposed at the boundary, and a point source is placed at the center of the upper surface. The convergence is presented in Table 5 for frequencies ranging from 1 to 30 Hz.

Whereas the iteration with ILU(0) hardly converges, not even for frequency $f = 1$ Hz, the complex shifted-Laplace preconditioner accelerates the iteration effectively. For low frequencies, the SV preconditioner outperforms the complex shifted-Laplace preconditioner, but the latter is faster as the frequency increases.

Even though multigrid can help reduce the number of iterations, it brings

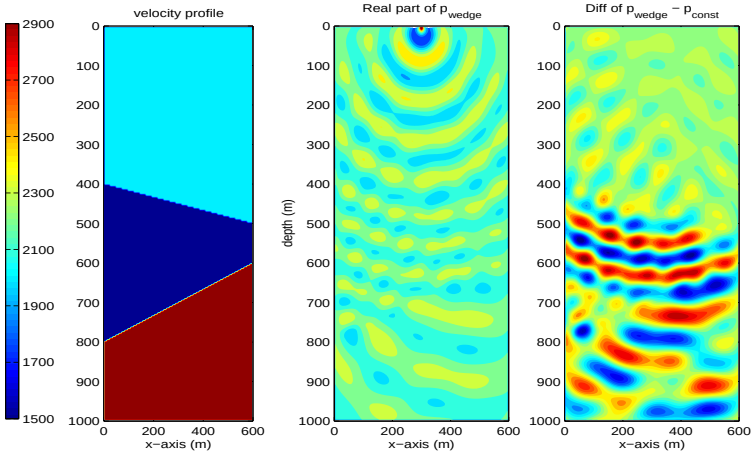

Figure 5: Wedge problem, $f = 20$ Hz. Domain and velocity profile (left), real part of the solution (middle), real part of difference between the solution from the wedge problem and constant medium (right). The reflection from the wedge interface is seen.

Table 4: Numerical results for the wedge problem. Number of iterations and (between parentheses) CPU time in sec. are shown for various frequencies f.

f (Hz)	10	20	30	40	50
grid	76×126	151×251	232×386	301×501	376×626
No-Prec	2379(9.5)	4057(84)	6907(333)	8248(658)	>10000
ILU(A,0)	571(3.9)	1339(40)	1917(139)	2443(293)	3287(651)
ILU(A,1)	239(1.8)	563(20)	832(70)	1120(155)	1418(195)
ILU(M_I,0)	529(3.5)	1066(31)	1718(118)	2173(250)	2959(539)
ILU(M_I,1)	235(1.7)	531(17)	787(61)	903(117)	1056(137)
ILU(M_{CSL},0)	485(3.3)	997(30)	1759(125)	2082(250)	2824(535)
ILU(M_{CSL},1)	212(1.7)	426(14)	664(55)	859(119)	1005(138)
MG(V(1,0))	48(0.8)	92(9)	132(33)	182(77)	213(141)
MG(V(1,1))	44(1.0)	91(12)	128(44)	182(103)	223(198)
M_{SV}	14(–)	45(–)	167(–)	830(–)	>2000(–)

only about 20% reduction in the CPU-time compared to ILU(1).

6 Conclusion

In this paper the complex shifted-Laplace preconditioner has been analyzed and improved. Two methods to approximately invert the complex shifted-Laplace preconditioner have been discussed, namely incomplete LU factorization and multigrid. In terms of the number of iterations, multigrid applied to the preconditioner inside Bi-CGSTAB results in a fast and robust method. Incomplete LU factorization is effective if some fill-in is allowed. With ILU(1) applied to the complex shifted-Laplace preconditioner a comparable performance to multigrid

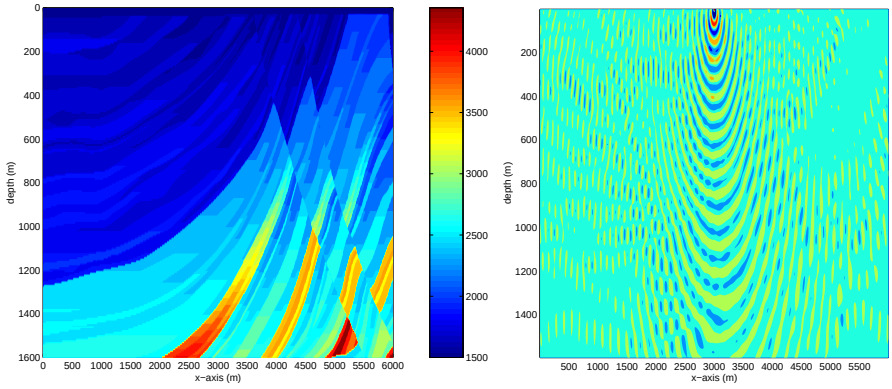

Figure 6: Marmousi problem. Velocity distribution in meter/s (left), real part of the solution for $f = 30$ Hz (right).

Table 5: Numerical results from Case 3 (a part of the Marmousi problem). Number of iterations and (in parentheses) CPU time in sec. are shown for various frequencies f.

f (Hz)	1	10	20	30
grid	751×201	751×201	1501×401	2001×534
No-Prec	17446(1375)	6623(538)	14687(4572)	–
ILU(A,0)	3058(365)	1817(219)	3854(1904)	–
ILU(A,1)	715(98)	740(107)	1706(988)	2391(2275)
ILU(M_I,0)	3282(373)	1654(190)	3645(1671)	–
ILU(M_I,1)	853(109)	755(98)	1718(860)	2444(2247)
ILU(M_{CSL},0)	2950(371)	1519(185)	3465(1618)	–
ILU(M_{CSL},1)	715(98)	743(107)	1369(763)	2010(1894)
MG(V(1,0))	16(9)	177(75)	311(537)	485(1445)
MG(V(1,1))	13(9)	169(94)	321(728)	498(1891)
M_{SV}	3	114	648	>2000

in terms of CPU time is often obtained.

The extension of multigrid to the complex linear systems under consideration has been done in a natural and straight forward way. With several multigrid components tested, we find the nine-point coarse grid stencil gives better convergence than the five-point coarse grid stencil obtained, for example, with half injection as the restriction operator. Fourier two-grid analysis confirms this numerical observation. The nine-point coarse grid stencil, however, leads to arithmetic work which is about one sixth more expensive than that of the five-point stencil on the coarse grids.

The CPU time results also suggest that multigrid for solving the preconditioner can be replaced by ILU(1). ILU(1) costs about three extra vectors to store some additional vectors. On the other hand, a matrix-free multigrid code can be written. The multigrid components have been chosen such that the method is well parallelizable.

Acknowledgment

The authors would like to thank Rene-Edouard Plessix and Wim A. Mulder of Shell International Exploration and Production, Rijswijk, The Netherlands, for fruitful discussions. The helpful comments of an anonymous referee are gratefully acknowledged.

References

[1] A. Bayliss, C.I. Goldstein, E. Turkel, An iterative method for Helmholtz equation, J. Comput. Phys., 49 (1983), pp. 443–457.

[2] A. Bourgeois, M. Bourget, P. Lailly, M. Poulet, P. Ricarte, R. Versteeg, Marmousi, model and data, in: R. Versteeg, G. Grau (Eds.), *The Marmousi*

Experience, Proceedings of the 1990 EAEG Workshop on Practical Aspects of Seismic Data Inversion, EAEG, Zeist, 1991, pp. 5–16.

[3] Y.A. Erlangga, C. Vuik, C.W. Oosterlee, On a class of preconditioners for the Helmholtz equation, Appl. Numer. Math., 50 (2004), pp.409–425.

[4] R.W. Freund, Conjugate gradient-type methods for linear systems with complex symmetric coefficients matrices, SIAM J. Sci. Comput. 13(1) (1992), pp. 425–448.

[5] M.J. Gander, F. Nataf, AILU for Helmholtz problems: a new preconditioner based on the analytical parabolic factorization, J. Comput. Acoustics, 9(4) (2001), pp. 1499–1506.

[6] W. Hackbusch, Multi-grid methods and applications, Springer, Berlin, 2003

[7] I. Harari, E. Turkel, Accurate finite difference methods for time-harmonic wave propagation, J. Comput. Phys., 119 (1995), pp. 252–270.

[8] R. Kechroud, A. Soulaimani, Y. Saad, Preconditioning techniques for the solution of the Helmholtz equation by the finite element method, in: Kumar et al. (Eds.) *2003 Workshop in wave phenomena in physics and engineering: new models, algorithms and Applications, May 18-21, 2003*, Springer Verlag, Berlin, 2003.

[9] A.L. Laird, M.B. Giles, Preconditioned iterative solution of the 2D Helmholtz equation, Report NA-02/12, Oxford University Computing Laboratory, 2002..

[10] D. Lahaye, H. De Gersem, S. Vandewalle, K. Hameyer, Algebraic multigrid for complex symmetric systems, IEEE Trans. Magn. 36(4) (2000), pp. 1535–1538.

[11] M.M. Monga Made, Incomplete factorization-based preconditionings for solving the Helmholtz equation, Int. J. Numer. Meth. Engng., 50, 2001, pp. 1077–1101.

[12] T.A. Manteuffel, S.V. Parter, Preconditioning and boundary conditions, SIAM J. Numer. Anal. 27(3) (1990), pp. 656–694.

[13] R.E. Plessix, W.A. Mulder, Separation-of-variables as a preconditioner for an iterative Helmholtz solver, Appl. Num. Math., 44 (2003), pp. 385–400.

[14] Y. Saad, M.H. Schultz, GMRES: A generalized minimal residual algorithm for solving nonsymmetric linear system, SIAM J. Sci. Comput. 7(3) (1986), pp. 856–869.

[15] Y. Saad, Iterative methods for sparse linear systems, 2^{th} edition, SIAM, 2003.

[16] U. Trottenberg, C.W. Oosterlee, A. Schüller, Multigrid, Academic Press, London, 2001.

[17] R.S. Varga, Matrix Iterative Analysis, Prentice-Hall, New Jersey, 1962

[18] H.A. van der Vorst, Bi-CGSTAB: A fast and smoothly converging variant of BiCG for the solution of nonsymmetric linear systems, SIAM J. Sci. Comput., 13(2) (1992), pp. 631–644.

[19] H.A. van der Vorst, J.B.M. Melissen, A Petrov-Galerkin type method for solving $Ax = b$, where A is symmetric complex, IEEE Trans. Magnetics, 26(2) (1990), pp.706–708.

[20] H.A. van der Vorst, C. Vuik, The superlinear convergence behaviour of GMRES, J. Comput. Appl. Math., 48 (1993), pp. 327–341.

[21] P.M. de Zeeuw, Matrix-dependent prolongations and restrictions in a black-box multigrid solver. J. Comp. Appl. Math., 33 (1990), pp. 1–27.